Available online at http://scik.org
Commun. Math. Biol. Neurosci. 2022, 2022:40
https://doi.org/10.28919/cmbn/7361
ISSN: 2052-2541

# TURING INSTABILITY OF A DIFFUSIVE PREDATOR-PREY MODEL ALONG WITH AN ALLEE EFFECT ON A PREDATOR

G. SANTHOSH KUMAR, C. GUNASUNDARI*

Department of Mathematics, SRM Institute of Science and Technology, Kattankulathur-603 203, India



**Abstract:** Modeling biological systems is a significant task in nature. This work concentrates on the relation between two prey species and one predator species model. Our interaction is based on a competition between two preys and one predator, with an additive Allee effect in the predator population. Many investigations have been done in stability properties of the population dynamics. However in this study, we demonstrated population instability as a result of the incorporating diffusive terms in the PDE system and we construct the amplitude equations of stationary patterns using the nonlinear multiple scale analysis approach and Taylor series expansion. Numerical results are also presented to validate our propositions.

**Keywords:** diffusive predator-prey model; turing instability; amplitude equation.

**2010 AMS Subject Classification:** 35B36, 92D40, 35G20.

## 1. Introduction

In the subject of real-world challenges, mathematical modeling in biology is highly interesting. Among the most fascinating topics is the product of the interplay between predator and prey in terrestrial ecosystems. When modeling a predator-prey system, a variety of mathematical approaches are utilized because Predation-mediated coexistence, vegetation size, logical grouping, execution and birth of species, competition, in comparability with respect to the population over

*Corresponding author

E-mail address: gunasunc1@srmist.edu.in

Received March 18, 2022

time, discrete, illness, and maturation delays, temperature variation, spatial dilution, eutrophication, geographic atmosphere diversity, and countable admittance period for extension seem to be just a few of the factors that can influence its propagation [1, 2]. Various computational predator-prey models were constructed by defining and suppressing the components that must be approached, and are caused by external types of equations: ordinary, partial, or functional differential equations, discrete or continuous, and so on [3, 4]. Several researchers developed the system and extended their works up to n dimensions. The correlation between two prey species and one predator species was the subject of this study. Our interaction is based on a competition between two preys and one predator, with an additive allee effect in the predator population and a Holling type II functional response in the prey population. Despite their limitations, Allee effects exist in small or sparse populations and are often thought to be prevalent in nature [5, 6]. In populations prone to Allee effects, population growth is reduced at low densities. Warder Clyde Allee, a biologist and animal ecologist at the University of Chicago, was fascinated with animal group behavior. Allee, a skilled observer of animal behavior, observed that many population growth of many species was hampered by under crowding rather than competition. For the animals in an environment, the Allee Effect causes a loss of biodiversity. Animals were dying as a result of this low-cost alteration in the ecosystem because they were unable to locate compatible partners, adequate food, or a healthy habitat.

$$\begin{aligned}
\frac{d\alpha}{dt} &= \eta_1\alpha(1-\alpha)-\sigma\alpha\beta-\frac{\omega_1\alpha\gamma}{1+\varsigma_1\alpha}\\
\frac{d\beta}{dt} &= \eta_2\beta(1-\beta)-\rho\alpha\beta-\frac{\omega_2\beta\gamma}{1+\varsigma_2\beta}\\
\frac{d\gamma}{dt} &= -\mu\gamma+\left(\frac{\rho_1\alpha\gamma}{1+\varsigma_1\alpha}+\frac{\rho_2\beta\gamma}{1+\varsigma_2\beta}\right)\left(\frac{\gamma}{\delta+\gamma}\right)
\end{aligned} \tag{1}$$

where $\alpha$, $\beta$ and $\gamma$ denote the first, second, and predator populations respectively. The intrinsic growth rates of the first and second prey populations are represented by $\eta_1$ and $\eta_2$. $\mu$ indicates the normal mortality rate of the predator. The competition coefficients of prey 2 on prey 1 and prey 1 on prey 2 are $\sigma$ and $\rho$ respectively. Because both prey and predator are simple to capture and handle, the Holling type II functional response is used to represent predation behavior (i.e) $\frac{\omega_1\alpha\gamma}{1+\varsigma_1\alpha}$ for the prey-1 and $\frac{\omega_2\beta\gamma}{1+\varsigma_2\beta}$ for the prey-2. $\rho_1$ and $\rho_2$ are the rate at which predation becomes predator growth.

In this paper, we produced diffusive terms in both the prey and predator population in the system. So that, we may not be able to guarantee that the population would remain stable indefinitely. This prompted us to consider a theoretical biologist Allen Turing's proposal for the occurrence of instability [7, 8]. Allen Turing had a substantial effect on the future of evolutionary computation, establishing a standardization of the ethics of algorithm and computing with the Turing machine, that might be termed a model of a general purpose computer. He is regarded as the founder of theoretical computer science and artificial intelligence. The pattern creation has recently received increased attention in the research of Turing bifurcation, amplitude equation, and secondary bifurcation. In section 2, Qianqian Zheng and Jianwei Shen discovered the dispersion of generic reactions with multi variable and derived the Turing instability condition. In section 3, they used the reaction-diffusion system with multi variable to get the amplitude equation [7, 9, 10]. Based on this, we derived the condition for turing bifurcation and amplitude equation of the diffusive predator prey interaction model. Finally, Turing spatial patterns for the diffusive predator prey system were generated [11].

## 2. Diffusive Predator Prey Model

Consider

$$
(2)\qquad \begin{cases}
\frac{\partial\alpha}{\partial t} & = d_1\Delta\alpha + \eta_1\alpha(1-\alpha) - \sigma\alpha\beta - \frac{\omega_1\alpha\gamma}{1+\varsigma_1\alpha}, x\in\Omega, t>0 \\
\frac{\partial\beta}{\partial t} & = d_2\Delta\beta + \eta_2\beta(1-\beta) - \rho\alpha\beta - \frac{\omega_2\beta\gamma}{1+\varsigma_2\beta}, x\in\Omega, t>0 \\
\frac{\partial\gamma}{\partial t} & = d_3\Delta\gamma - \mu\gamma + \left(\frac{\rho_1\alpha\gamma}{1+\varsigma_1\alpha} + \frac{\rho_2\beta\gamma}{1+\varsigma_2\beta}\right)\left(\frac{\gamma}{\delta+\gamma}\right) x\in\Omega, t>0 \\
\frac{\partial\alpha}{\partial t} & = \frac{\partial\beta}{\partial t} = \frac{\partial\gamma}{\partial t} = 0
\end{cases}
$$

where $d_1$, $d_2$ and $d_3$ are the positive diffusive coefficients of first, second prey and the predator respectively and $\Delta\alpha = \frac{\partial^2\alpha}{\partial x^2}$, $\Delta\beta = \frac{\partial^2\beta}{\partial x^2}$, $\Delta\gamma = \frac{\partial^2\gamma}{\partial x^2}$, where $\Delta = \frac{\partial^2}{\partial x^2}$ is a Laplacian operator.

Turing instability appears when a spatially homogeneous linear progression becomes unstable mainly attributed to small amplitude non - homogeneous disturbance locally. Consider the presence of an endemic equilibrium $E^* = (\alpha^*, \beta^*, \gamma^*)$, then linearize to get the Jacobian matrix below by including the wave number k.

$$J(P_i)=\begin{pmatrix} A^*-k^2d_1 & -\sigma\alpha & \frac{-\omega_1\alpha}{1+\varsigma_1\alpha} \\ -\rho\beta & B^*-k^2d_2 & \frac{-\omega_2\beta}{1+\varsigma_2\beta} \\ \frac{\rho_1\gamma}{(1+\varsigma_1\alpha)^2}\frac{\gamma}{\delta+\gamma} & \frac{\rho_2\gamma}{(1+\varsigma_2\beta)^2}\frac{\gamma}{\delta+\gamma} & C^*-k^2d_3 \end{pmatrix}$$

where,

$$\begin{aligned} A^* &= \eta_1-2\eta_1\alpha-\sigma\beta-\frac{\omega_1\gamma}{(1+\varsigma_1\alpha)^2} \\ B^* &= \eta_2-2\eta_2\beta-\rho\alpha-\frac{\omega_2\gamma}{(1+\varsigma_2\beta)^2} \qquad (3) \\ C^* &= -\mu+\frac{\rho_1\alpha\gamma(2\delta+\gamma)}{(1+\varsigma_1\alpha)(\delta+\gamma)^2}+\frac{\rho_2\beta\gamma(2\delta+\gamma)}{(1+\varsigma_1\beta)(\delta+\gamma)^2} \end{aligned}$$

Then the characteristic equation is given by,

$$\lambda^3+p(k^2)\lambda^2+q(k^2)\lambda+r(k^2)=0 \qquad (4)$$

where, $p(k^2)=-k^2(d_1+d_2+d_3)+(A^*+B^*+C^*)$,

$$\begin{aligned} q(k^2) &= -3d_1d_2d_3k^6+3(d_1d_2C^*+d_1d_3B^*+d_2d_3A^*)k^4 \\ &+\left[d_3\sigma\rho\alpha\beta-\left(\frac{d_1\rho_2\omega_2\beta\gamma^2}{(1+\varsigma_2\beta)^2(\delta+\gamma)}+\frac{d_2\rho_1\omega_1\alpha\gamma^2}{(1+\varsigma_1\alpha)^2(\delta+\gamma)}+3(d_1B^*C^*+d_2A^*C^*+d_3A^*B^*)\right)\right]k^2 \\ &+3B^*A^*C^*-C^*\sigma\rho\alpha\beta+\frac{A^*\rho_2\omega_2\beta\gamma^2}{(1+\varsigma_2\beta)^3(\delta+\gamma)}+\frac{B^*\rho_1\omega_1\alpha\gamma^2}{(1+\varsigma_1\alpha)^3(\delta+\gamma)} \\ r(k^2) &= d_1d_2d_3k^6-(A^*d_2d_3+B^*d_1d_3+C^*d_1d_2)k^4 \\ &-\left[\sigma\rho\alpha\beta d_3-\left(A^*C^*d_2+A^*B^*d_3+B^*C^*d_1+\frac{d_1\rho_2\omega_2\beta\gamma^2}{(1+\varsigma_2\beta)^3(\delta+\gamma)}+\frac{d_2\rho_1\omega_1\alpha\gamma^2}{(1+\varsigma_1\alpha)^3(\delta+\gamma)}\right)\right]k^2 \\ &+\sigma\rho\alpha\beta C^*-A^*B^*C^*+\frac{A^*\rho_2\omega_2\beta\gamma^2}{(1+\varsigma_2\beta)^3(\delta+\gamma)}+\frac{B^*\rho_1\omega_1\alpha\gamma^2}{(1+\varsigma_1\alpha)^3(\delta+\gamma)}+\frac{\sigma\rho_1\omega_2\alpha\beta\gamma^2}{(1+\varsigma_1\alpha)^2(1+\varsigma_2\beta)(\delta+\gamma)} \\ &+\frac{\rho\rho_2\omega_1\alpha\beta\gamma^2}{(1+\varsigma_1\alpha)(1+\varsigma_2\beta)^2(\delta+\gamma)} \end{aligned}$$

where $p(k^2)<0$ if $A^*+B^*+C^*>K^2(d_1+d_2+d_3)$. Eqn (2) is stable if $tr(J(P_i))<0$ and $det(J(P_i))>0$. If it violates $det(J(P_i))<0$, then the system is unstable. So that the expression $r(k^2)$ can be rewritten as,

$$r(k^2)=r_3(k^2)^3+r_2(k^2)^2+r_1(k^2)+r_0 \qquad (5)$$

where $r_3=d_1d_2d_3>0$ as $d_1=d_2=d_3>0$, $r_2=-(A^*d_2d_3+B^*d_1d_3+C^*d_1d_2)<0$, $r_1=-\left[\sigma\rho\alpha\beta d_3-\left(A^*C^*d_2+A^*B^*d_3+B^*C^*d_1+\frac{d_1\rho_2\omega_2\beta\gamma^2}{(1+\varsigma_2\beta)^3(\delta+\gamma)}+\frac{d_2\rho_1\omega_1\alpha\gamma^2}{(1+\varsigma_1\alpha)^3(\delta+\gamma)}\right)\right]<0$ if

$\sigma\rho\alpha\beta d_3 > \left(A^*C^*d_2 + A^*B^*d_3 + B^*C^*d_1 + \frac{d_1\rho_2\omega_2\beta\gamma^2}{(1+\varsigma_2\beta)^3(\delta+\gamma)} + \frac{d_2\rho_1\omega_1\alpha\gamma^2}{(1+\varsigma_1\alpha)^3(\delta+\gamma)}\right)$,

$$r_0 = \sigma\rho\alpha\beta C^* - \left(A^*B^*C^* + \frac{A^*\rho_2\omega_2\beta\gamma^2}{(1+\varsigma_2\beta)^3(\delta+\gamma)} + \frac{B^*\rho_1\omega_1\alpha\gamma^2}{(1+\varsigma_1\alpha)^3(\delta+\gamma)} + \frac{\sigma\rho_1\omega_1\alpha\beta\gamma^2}{(1+\varsigma_1\alpha)^2(1+\varsigma_2\beta)(\delta+\gamma)} + \frac{\rho\rho_2\omega_1\alpha\beta\gamma^2}{(1+\varsigma_1\alpha)(1+\varsigma_2\beta)^2(\delta+\gamma)}\right) < 0 \text{ if } \sigma\rho\alpha\beta C^* < (A^*B^*C^* + \mathbb{H})$$

where $\mathbb{H} = A^*B^*C^* + \frac{A^*\rho_2\omega_2\beta\gamma^2}{(1+\varsigma_2\beta)^3(\delta+\gamma)} + \frac{B^*\rho_1\omega_1\alpha\gamma^2}{(1+\varsigma_1\alpha)^3(\delta+\gamma)} + \frac{\sigma\rho_1\omega_1\alpha\beta\gamma^2}{(1+\varsigma_1\alpha)^2(1+\varsigma_2\beta)(\delta+\gamma)} + \frac{\rho\rho_2\omega_1\alpha\beta\gamma^2}{(1+\varsigma_1\alpha)(1+\varsigma_2\beta)^2(\delta+\gamma)}$. Therefore

$$r(k^2) = r_3(k^2)^3 - r_2(k^2)^2 - r_1(k^2) - r_0 \tag{6}$$

So that, $r(k^2) < 0$ if

$$r_3 < (r_0 + r_1 + r_2) \tag{7}$$

If all other requirements are met, (6) is an implicit formula for Turing Bifurcation Spatial Patterns.

## 3. Amplitude Equation

The equilibria around the instability threshold is not stable, the eigenvalues connected to the essential modes are near zero, and these modes are gradually changing, while the modes that are critically weak, therefore only the interruptions with k near $k_T$ must be considered. The amplitude equations are derived via multiple scale analysis. The solution of systems could be extended as,

$$C = C_0 + (Z_1e^{kr} + Z_2e^{2kr} + Z_3e^{3kr}) + \text{Complex Conjugate} \tag{8}$$

We can write system (8) as

$$\frac{\partial c}{dt} = Lc + N(c,c) \tag{9}$$

where $c = \begin{pmatrix} \alpha \\ \beta \\ \gamma \end{pmatrix}$ is the variable, $L = A + D\nabla^2$ is the linear operator, such that

$$L = \begin{pmatrix} \eta_1 - \sigma_1\beta - \frac{\omega_1\gamma}{1+\varsigma_1\alpha} + d_1\nabla^2 & -\sigma\alpha & \frac{-\omega_1\alpha}{1+\varsigma_1\alpha} \\ -\rho\beta & \eta_2 - \rho_2\alpha - \frac{\omega_2\gamma}{1+\varsigma_2\beta} + d_2\nabla^2 & \frac{-\omega_2\beta}{1+\varsigma_2\beta} \\ \frac{\rho_1\gamma^2}{(1+\varsigma_1\alpha)}\frac{1}{\delta+\gamma} & \frac{\rho_2\gamma^2}{(1+\varsigma_2\beta)}\frac{1}{\delta+\gamma} & -\mu + d_3\nabla^2 \end{pmatrix}$$

and $N = \begin{pmatrix} \eta_1\alpha^2 \\ 0 \\ 0 \end{pmatrix}$ is the non-linear term. When $\mu$ is close to $\mu_c$, we must analyze the dynamical behavior, and then we must expand as

$$\mu_c - \mu = \varepsilon\mu_1 + \varepsilon^2\mu_2 + ...$$

where $\varepsilon$ is a sufficiently small parameter. The series forms of C and N are expanded.

$$C = \begin{pmatrix} \alpha \\ \beta \\ \gamma \end{pmatrix} = \begin{pmatrix} \alpha_1 \\ \beta_1 \\ \gamma_1 \end{pmatrix} \varepsilon + \begin{pmatrix} \alpha_2 \\ \beta_2 \\ \gamma_2 \end{pmatrix} \varepsilon^2 + ...$$

$$N = \begin{pmatrix} -\eta_1\alpha_1^2\varepsilon^2 + (-\eta_1\alpha_1\beta_1)\varepsilon^3 + 0(\varepsilon^4) \\ 0 \\ 0 \end{pmatrix}$$

L can be written as

$$L = L_c + (\mu_c - \mu)M \tag{10}$$

Let $T_0 = t$, $T_1 = \varepsilon t$, $T_2 = \varepsilon^2 t$, such that $\frac{\partial}{\partial t} = \frac{\partial}{\partial T_0} + \varepsilon\frac{\partial}{\partial T_1} + \varepsilon^2\frac{\partial}{\partial T_2} + ...$ Amplitude is a slow variable, while $T_i$ is a dependent variable. We have that as a basis for calculating time,

$$\frac{\partial W}{\partial t} = \varepsilon\frac{\partial W}{\partial T_1} + \varepsilon^2\frac{\partial W}{\partial T_2} + ...$$

We may get three equations by substituting the previous equations into (2) and extending (2) according to different orders of $\varepsilon$:

$$\varepsilon : L_c \begin{pmatrix} \alpha_1 \\ \beta_1 \\ \gamma_1 \end{pmatrix} = 0$$

$$\varepsilon^2 : L_c \begin{pmatrix} \alpha_2 \\ \beta_2 \\ \gamma_2 \end{pmatrix} = \frac{\partial}{\partial T_1} \begin{pmatrix} \alpha_1 \\ \beta_1 \\ \gamma_1 \end{pmatrix} - \mu_1 M \begin{pmatrix} \alpha_1 \\ \beta_1 \\ \gamma_1 \end{pmatrix} - \begin{pmatrix} -\eta_1 \alpha_1^2 \\ 0 \\ 0 \end{pmatrix}$$

$$\varepsilon^3 : L_c \begin{pmatrix} \alpha_3 \\ \beta_3 \\ \gamma_3 \end{pmatrix} = \frac{\partial}{\partial T_1} \begin{pmatrix} \alpha_2 \\ \beta_2 \\ \gamma_2 \end{pmatrix} + \frac{\partial}{\partial T_2} \begin{pmatrix} \alpha_1 \\ \beta_1 \\ \gamma_1 \end{pmatrix} - \mu_1 M \begin{pmatrix} \alpha_2 \\ \beta_2 \\ \gamma_2 \end{pmatrix} - \mu_2 M \begin{pmatrix} \alpha_1 \\ \beta_1 \\ \gamma_1 \end{pmatrix}$$
$$- \begin{pmatrix} -\eta_1 \alpha_1^2 \\ 0 \\ 0 \end{pmatrix} \begin{pmatrix} \alpha_1 \\ \beta_1 \\ \gamma_1 \end{pmatrix} \begin{pmatrix} \alpha_2 \\ \beta_2 \\ \gamma_2 \end{pmatrix} - \begin{pmatrix} -\eta_1 \alpha_1 \beta_1 \\ 0 \\ 0 \end{pmatrix}$$

The example of the first order of $\varepsilon$ is first considered. $(\alpha_1, \beta_1, \gamma_1)^T$ is the linear combination of the eigenvectors that corresponds to the eigenvalue zero, since Lc is the linear operator of the system at the onset. Since then, this has occurred.

$$\begin{pmatrix} \alpha \\ \beta \\ \gamma \end{pmatrix} = \begin{pmatrix} x_1 \\ y_1 \\ z_1 \end{pmatrix} e^{k_1 r} + \begin{pmatrix} x_2 \\ y_2 \\ z_2 \end{pmatrix} e^{2k_2 r} + \begin{pmatrix} x_3 \\ y_3 \\ z_3 \end{pmatrix} e^{3k_3 r} + \text{complex conjugate}$$

and are able to obtain that $x_i = By_i$. Let $x_i = B$ by assuming $y_i = 1$ and $z_i = 0$ then

$$\begin{pmatrix} \alpha_1 \\ \beta_1 \\ \gamma_1 \end{pmatrix} = \begin{pmatrix} B \\ 1 \\ 0 \end{pmatrix} (W_1 e^{k_1 r} + W_2 e^{2k_2 r} + W_3 e^{3k_3 r}) + \text{complex conjugate}$$

Let us consider the case of $\varepsilon^2$ now. The vector function of the right hand of the preceding equation must be orthogonal to the zero eigenvectors of operator ${L_c}^+$, according to the Fredholm solubility condition. The adjoint operator ${L_c}^+$ has zero eigenvectors such that $\begin{pmatrix} 1 \\ A \\ 0 \end{pmatrix} e^{-iK_i r}$ + Complex Conjugate. From the orthogonality criterion, it can be shown that, $\begin{pmatrix} 1 \\ A \\ 0 \end{pmatrix} e^{-ik_i r}$

$L_c \begin{pmatrix} \alpha_2 \\ \beta_2 \\ \gamma_2 \end{pmatrix} = 0$. Another example we may get by analyzing $e^{ik_1r}$ just in the following is by modifying the subscript. It is derived from the orthogonality constraint.

$$(A+B)\frac{\partial W_1}{\partial T_1} = [b_{11}B + b_{12} + (b_{21}B + b_{22})A]W_1 - (Ab+Bb)\eta_1\alpha_1^2\overline{W_2W_3} \tag{11}$$

One can get the same results by employing the same procedures,

$$\begin{pmatrix} \alpha_2 \\ \beta_2 \\ \gamma_2 \end{pmatrix} = \begin{pmatrix} a_0 \\ b_0 \\ c_0 \end{pmatrix} + \begin{pmatrix} a_i \\ b_i \\ c_i \end{pmatrix} e^{ik_ir} + \begin{pmatrix} a_{ii} \\ b_{ii} \\ c_{ii} \end{pmatrix} e^{i2k_ir} + \begin{pmatrix} a_{12} \\ b_{12} \\ c_{12} \end{pmatrix} e^{i(k_1-k_2)r} + \begin{pmatrix} a_{23} \\ b_{23} \\ c_{23} \end{pmatrix} e^{i(k_2-k_3)r} + \begin{pmatrix} a_{31} \\ b_{31} \\ c_{31} \end{pmatrix} e^{i(k_3-k_1)r} + \text{Complex Conjugate}$$

We have that in the case of $\varepsilon^3$. We may obtain by using the Fredholm solubility condition once again.

$$\begin{aligned} (A+B)(\frac{\partial z}{\partial T_1} + \frac{\partial z}{\partial T_2}) = (\mu_1 z_1 + \mu_2 W_1)[b_{11}B + b_{12} + (b_{21}B + b_{22})A] - (Ab+Bb)\eta_1\alpha_1^2 \\ (\overline{Z_2W_3} + \overline{Z_3W_2}) - (bAB + bB^2 + bA + bB)\eta_1\alpha_1\beta_1 \\ (|\, W_1\,|^2 + |\, W_2\,|^2 + |\, W_3\,|^2)W_1 \end{aligned} \tag{12}$$

Calculations are used to derive the coefficient expressions, $\mu_0 = A+B$, $\mu^* = \mu_c - \mu$, $h = -(bA+bB)\eta_1\alpha_1^2$ and $g = (bAB + bB^2 + bA + bB)\eta_1\alpha_1\beta_1$. As a result, the amplitude equation is as follows:

$$\begin{aligned} \mu_0\frac{\partial W_1}{\partial t} &= \mu^* W_1 + h\overline{W_2W_3} - (g|\, W_1\,|^2 + g|\, W_2\,|^2 + g|\, W_3\,|^2)W_1 \\ \mu_0\frac{\partial W_2}{\partial t} &= \mu^* W_2 + h\overline{W_1W_3} - (g|\, W_2\,|^2 + g|\, W_1\,|^2 + g|\, W_3\,|^2)W_2 \\ \mu_0\frac{\partial W_3}{\partial t} &= \mu^* W_3 + h\overline{W_2W_1} - (g|\, W_3\,|^2 + g|\, W_2\,|^2 + g|\, W_1\,|^2)W_3 \end{aligned} \tag{13}$$

## 4. Numerical Simulation

The unique approach of spatial patterns reduces the size of the differential in space and it also uses the homotopy in time to derive the analytical expression with physical parameters. It will make to analyze the impact of parameter variations on Turing pattern construction much easier. When the number of iterations increases, we get the alternative pattern forms of system (2). We observed how small changes in the self-diffusion parameters $d_1$ and $d_2$ in one dimension may lead to huge alterations in the observational mechanisms of solutions. When the diffusion coefficient constraints are elevated, we include a fundamental transformation in the dynamics of the system from fragmented to standard orientation. Around the spatially diffusive predator prey model system, we detected Turing patterns and implemented a structural analysis combining amplitude equations and multiple-scale analysis. We found three types of Turing patterns near the bifurcation threshold parameter, namely spots, spots-stripes, and stripes.

We investigate our model with the below set of parameter values, $\rho = 0.1$, $\omega_1 = 1$, $\varsigma_1 = 0.0001$, $\eta_2 = 0.5$, $\varsigma_2 = 0.03$, $\mu = 1$, $\rho_1 = 0.1$ and $\delta = 0.02$.

We can see that the spatial patterns of prey were spread in the form of spot patterns at first, as depicted in Figure 1(A). The population is discovered in the form of a mixture of spots and stripe patterns when the value of iteration fluctuates, as illustrated in Figure 1(B) and Figure 1(C). Similarly, the second prey population's spatial patterns take the shape of spot patterns Figure 2(A). As the iteration progresses, a blend of spot and spatial patterns emerges Figure 2(B). We noticed that there aren't many pattern changes at the maximum iteration, as illustrated in Figure 2(C).

Figure (3) shows the effects of extra parameters supplied to a predator on the system dynamics of spatial model iterations are depicted in (A), (B), and (C). The predator population density is spread in places. When we raise the value of the parameter, however the evolution of the spatial pattern changes dramatically, as it transforms to a stripe-like pattern from a spot pattern.

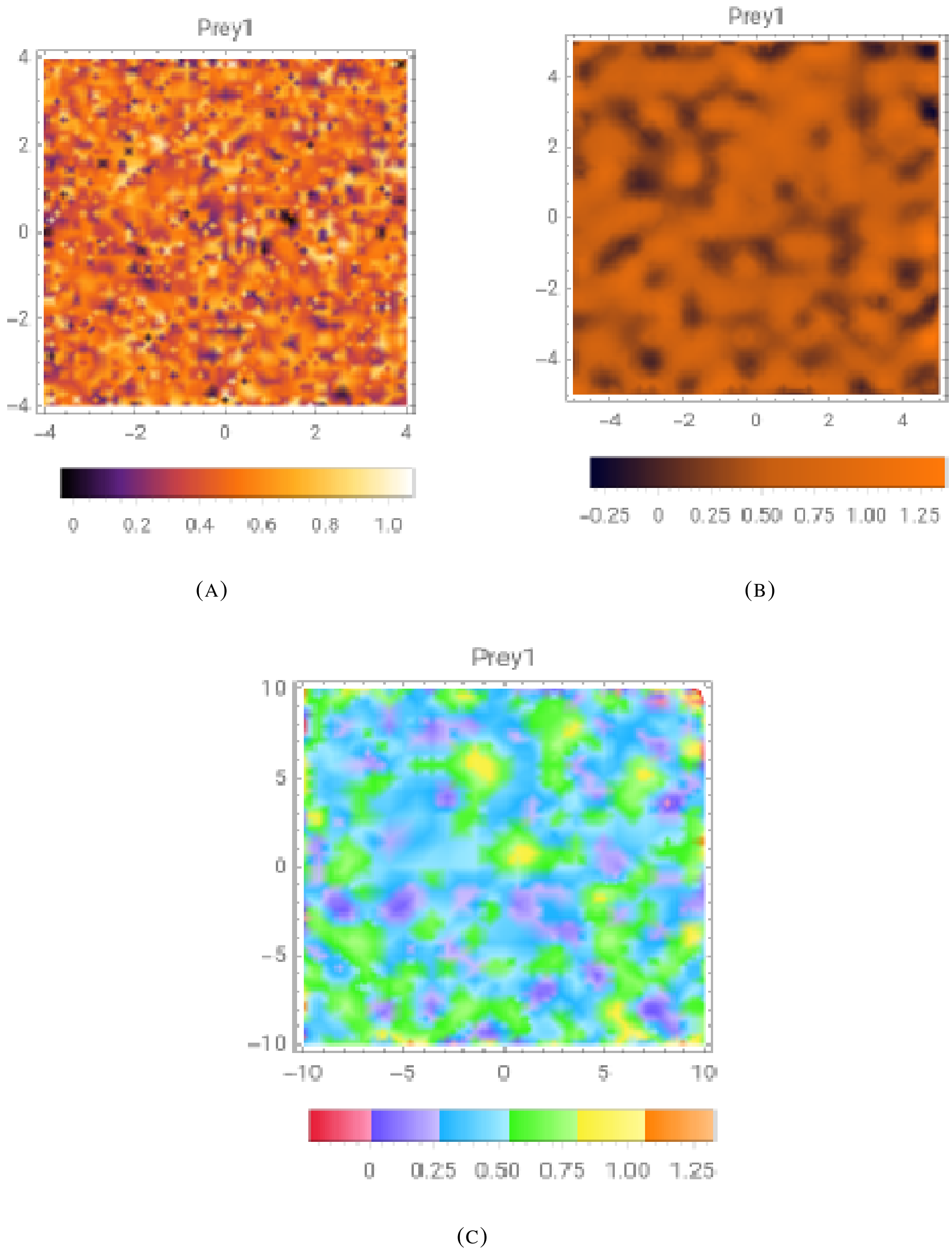


FIGURE 1. Turing patterns showing the spatial temporal development of several sorts of patterns produced by $\alpha$ in the diffusive model on an XY-plane, given different parameter values $d_1 = 3.1$, $d_1 = 3.0$, and $d_1 = 0.2$. The values of other parameters have already been given.

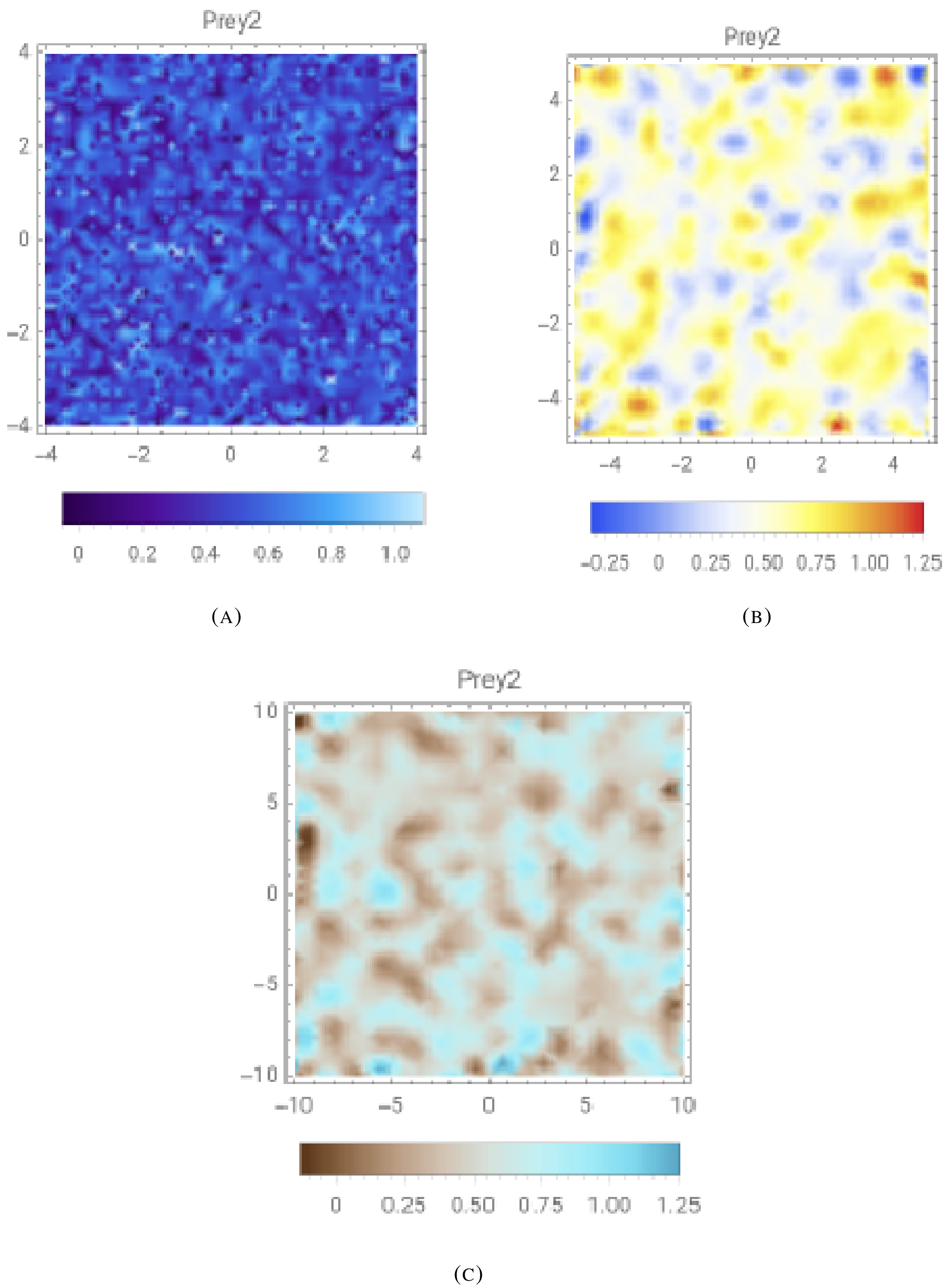


FIGURE 2. In the XY-Plane of the diffusive model, snapshots of turing patterns of the temporal evolution of second prey population is shown here for the different parameter set of values $d_2 = 15.2$, $d_2 = 0.2$ and $d_2 = 0.01$.

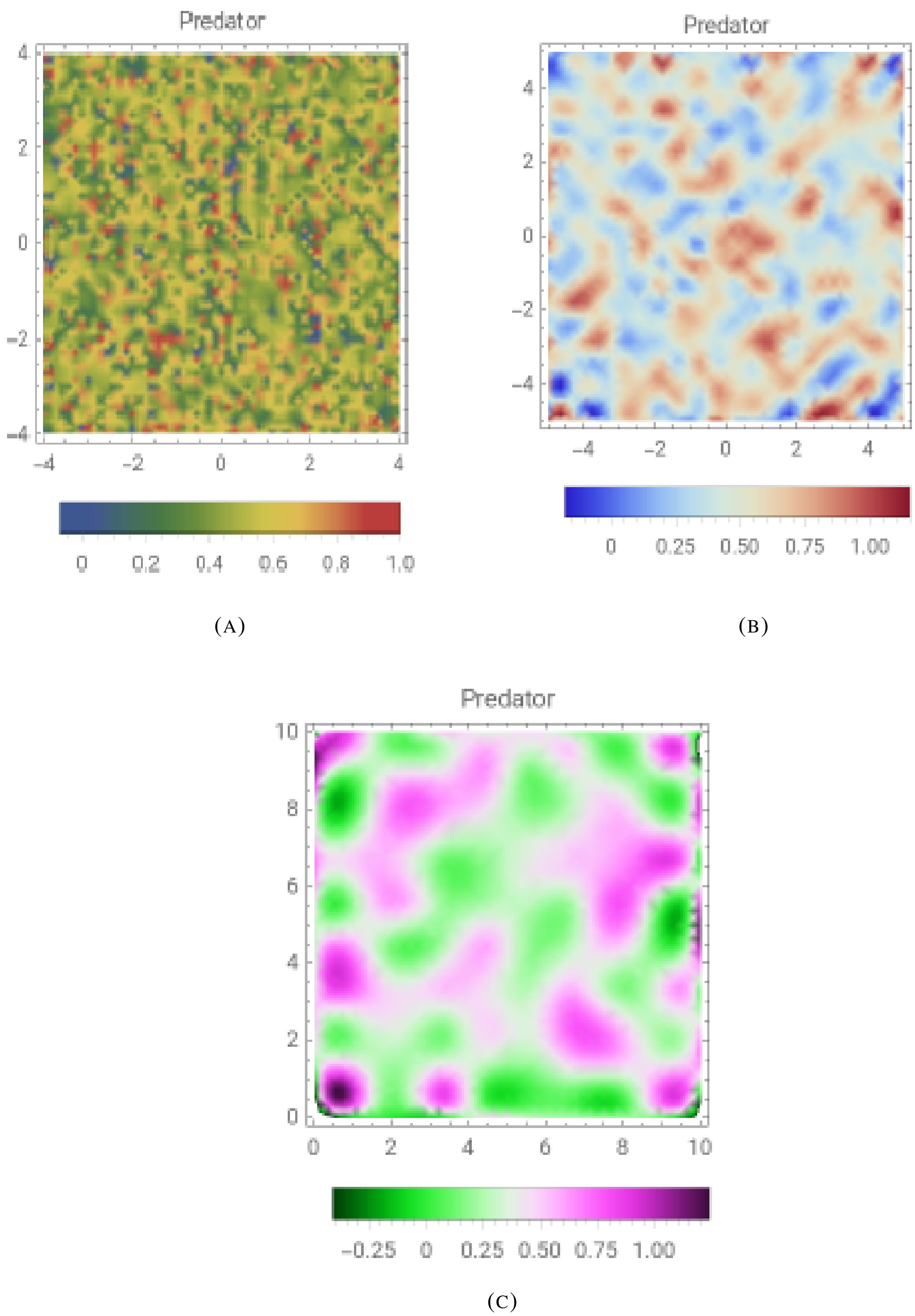


FIGURE 3. Evolution of spatial temporal turing patterns only for the predator in the diffusive model. Whereas, $d_3 = 0.3$, $d_3 = 0.2$ and $d_3 = 0.0002$ respectively.

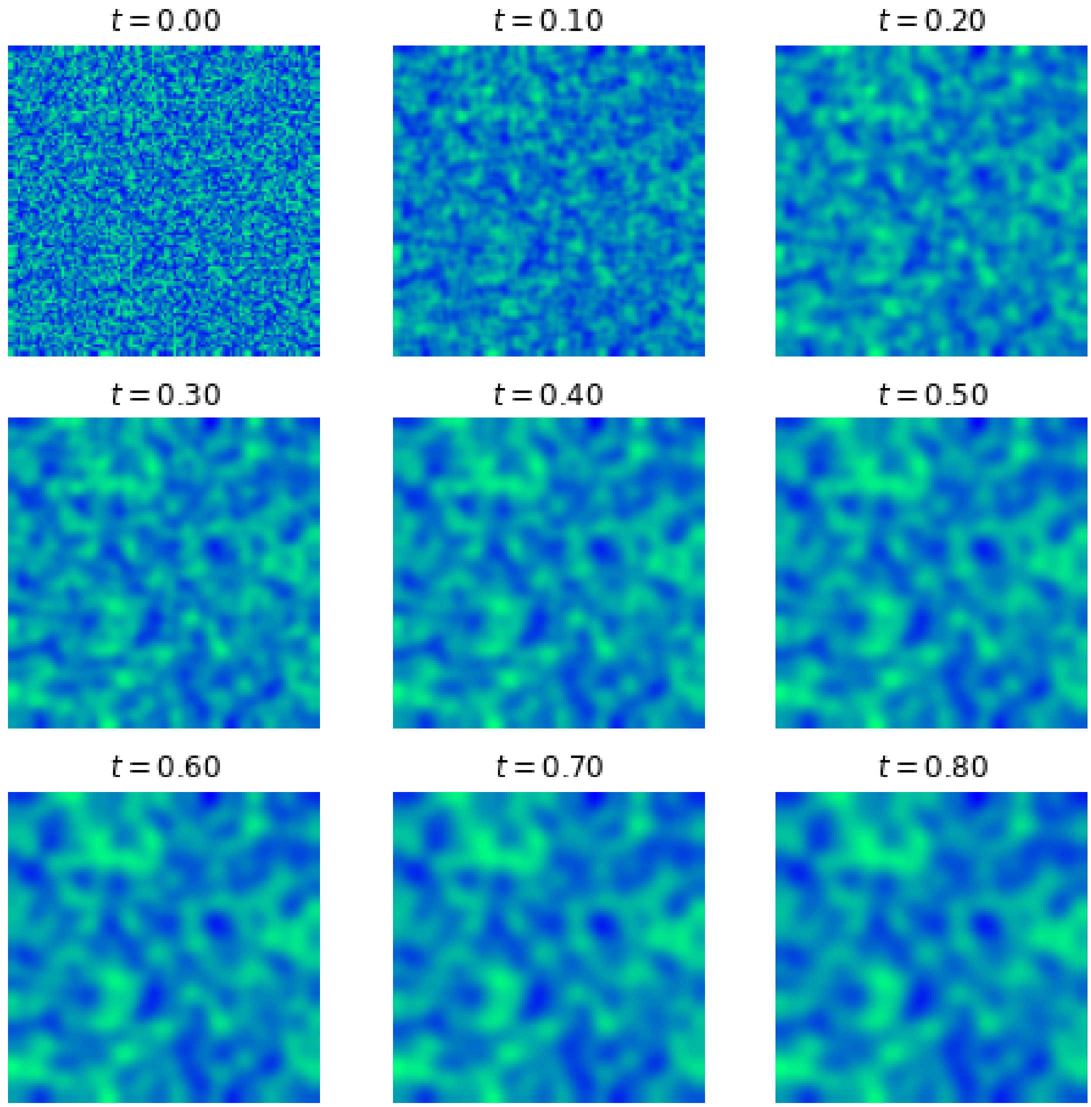


(A)

FIGURE 4. Frames of different spatial patterns of the first prey is shown, when time varies (t)= 0.1, 0.2, 0.3, ..., 0.8.

Turing patterns in homotopy series solutions are impacted by the wave number and are sensitive to the first guess solution. For various values of time such as t= 0.1, 0.2, 0.3,..., 0.8, different forms of Turing pattern may be created for the prey population using Mathematica software or experimental data simulation of the structure of the solution. As the time value increases, spot patterns become spatial pattern graphs. As shown in accompanying illustration.

## 5. Conclusion

This discussion proposed a detailed study and mathematical modeling of the Turing instability with two prey and one predator scenario with Allee effect. After running a series of numerical simulations, it was discovered that reaction diffusion systems using a three-dimensional method had rich spatial dynamics. We also used multiple scale analysis in theory to construct the amplitude equation, which can be used to tackle various pattern creation issues with many variables in the future. In the extant literature, there are fewer research on pattern development for three-species models, and significantly fewer chances for models with non local interactions. We looked at the effects of random dispersion and non local inter species communications on the evolution of a two-prey, one-predator system in this research. In addition, we provided numerical simulations to test our theoretical predictions and to investigate rich complex dynamical phenomena that are beyond the scope of linear analysis. The current work used two prey and one predator species to capture prey predator interactions as well as diffusive terms, while also taking into account better suitable functional responses Holling type I and discrete time delay to make the investigation more ecologically feasible and demanding. These fascinating as well as difficult themes will be addressed in future projects.

## Conflict of Interests

The author(s) declare that there is no conflict of interests.

## References

[1] G. Chandrasekar, S.M. Boulaaras, S. Murugaiah, A.J. Gnanaprakasam, B.B. Cherif, Analysis of a predator-prey model with distributed delay, J. Funct. Spaces. 2021 (2021), 9954409. https://doi.org/10.1155/2021/9954409.

[2] M. Senthilkumaran, C. Gunasundari, Stability and Hopf bifurcation in a delayed predator-prey system with parental care for predators, J. Math. Comput. Sci. 7 (2017), 495-521

[3] D. Savitri, A. Suryanto, W.M. Kusumawinahyu, Abadi, Dynamics of two preys - one predator system with competition between preys, J. Phys.: Conf. Ser. 1562 (2020), 012010. https://doi.org/10.1088/1742-6596/1562/1/012010.

[4] D. Savitri, A. Suryanto, W.M. Kusumawinahyu, Abadi, A dynamics behaviour of two predators and one prey interaction with competition between predators, IOP Conf. Ser.: Mater. Sci. Eng. 546 (2019), 052069. https://doi.org/10.1088/1757-899X/546/5/052069.

[5] A.A. Shaikh, H. Das, An eco-epidemic predator–prey model with Allee effect in prey, Int. J. Bifurcation Chaos. 30 (2020), 2050194. https://doi.org/10.1142/S0218127420501941.

[6] P.S. Mandal, U. Kumar, K. Garain, R. Sharma, Allee effect can simplify the dynamics of a prey-predator model, J. Appl. Math. Comput. 63 (2020), 739–770. https://doi.org/10.1007/s12190-020-01337-4.

[7] Q. Zheng, J. Shen, Turing instability and amplitude equation of reaction-diffusion system with multivariable, Math. Probl. Eng. 2020 (2020), 1381095. https://doi.org/10.1155/2020/1381095.

[8] K. Manna, V. Volpert, M. Banerjee, Dynamics of a diffusive two-prey-one-predator model with nonlocal intra-specific competition for both the prey species, Mathematics. 8 (2020), 101. https://doi.org/10.3390/math8010101.

[9] Q. Zheng, J. Shen, Pattern formation in the FitzHugh–Nagumo model, Computers Math. Appl. 70 (2015), 1082–1097. https://doi.org/10.1016/j.camwa.2015.06.031.

[10] T. Singh, K. Shrivastava, A. Kumar, R. Dubey, V. Narayan Mishra, Pattern formation of prey–predator system with schooling behavior via amplitude equation, Adv. Math.: Sci. J. 9 (2020), 9697–9712. https://doi.org/10.37418/amsj.9.11.77.

[11] G. Gu, H. Peng, Numerical simulation of reaction-diffusion systems of turing pattern formation, Int. J. Modern Nonlinear Theory Appl. 04 (2015), 215–225. https://doi.org/10.4236/ijmnta.2015.44016.